Pig Ulnar Nerve Recording with Sinusoidal and Temporal Interference Stimulation

Leen Jabban, Mafalda Ribeiro, Felipe Rettore Andreis, Thomas Gomes Nørgaard dos Santos Nielsen, and Benjamin W. Metcalfe

Abstract— Temporal interference stimulation has been suggested as a method to reach deep targets during transcutaneous electrical stimulation. Despite its growing use in transcutaneous stimulation therapies, the mechanism of its operation is not fully understood. Recent efforts to fill that gap have focused on computational modelling, in vitro and in vivo experiments relying on physical observations – e.g., sensation or movement. This paper expands the current range of experimental methods by demonstrating in vivo extraneural recordings from the ulnar nerve of a pig while applying temporal interference stimulation at a location targeting a distal part of the nerve. The main aim of the experiment was to compare neural activation using sinusoidal stimulation (100 Hz, 2 kHz, 4 kHz) and temporal interference stimulation (2 kHz and 4 kHz). The recordings showed a significant increase in the magnitude of stimulation artefacts at higher frequencies. While those artefacts could be removed and provided an indication of the depth of modulation, they resulted in the saturation of the amplifiers, limiting the stimulation currents and amplifier gains used. The results of the 100 Hz sine wave stimulation showed clear neural activity correlated to the stimulation waveform. However, this was not observed with temporal interference stimulation. The results suggest that, despite its greater penetration, higher currents might be required to observe a neural response with temporal interference stimulation, and more complex artefact rejection techniques may be required to validate the method.

I. INTRODUCTION

The concept of temporal interference (TI) stimulation (or interferential stimulation) dates back to the 1950s as a method to overcome skin impedance and stimulate deeper tissue not reached with traditional transcutaneous stimulation therapies [1]. However, despite its widespread use, the underlying mechanisms of TI are not yet well understood. TI was recently re-visited by Grossman et al. as an approach to achieve deep brain stimulation, and it has since gained increased research attention both for brain and peripheral nerve stimulation [2], [3].

The basic principle of TI stimulation is that the electrical stimulation via two kilohertz-frequency (f_1 and f_2) sinusoidal waves that differ by Δf results in areas of temporal interference where an envelope waveform is formed at a frequency of Δf. The magnitude of the envelope is greatest at locations where both waveforms have the same magnitude (e.g., the centre of a uniform, homogeneous structure where f_1 and f_2 are applied at opposite ends). TI has, therefore, been proposed as a method to target deeper tissues based on the assumption that neurons are more likely to be activated by the lower frequency envelope than by the high-frequency source waveforms, resulting in more comfortable stimulation as fewer nerve endings are stimulated in the skin [4].

In-vivo experiments that investigate TI relied on observations such as the movement of the whiskers [2] or diaphragm [5]. Those experiments confirmed the relevance of using the modulation envelope as a metric to determine the stimulation location. However, Mirzakahlili et al. used computational modelling to demonstrate that the modulation envelope might not be an accurate metric to assess activation of the nerves, particularly along the length of the nerve [6].

Overall, in-vivo experiments tend to show promising results while simulation results (on a human scale) vary and tend to be less promising, with many showing that TI stimulation fails to activate deep nerves due to the increased currents required [7]. Moreover, the reliance on movement observations in in-vivo experiments may fail to show the effect of TI on the surrounding areas (for example, simulation has shown areas of conduction block and tonic activation [6]).

To investigate the mechanism of TI stimulation at a deeper level, in vitro experiments have been conducted on rat hippocampal slices [8] and rat dorsal rootlets [9]. However, to the best of our knowledge, no in vivo experiments have been conducted at the intermediate stage, looking at electroneurogram (ENG) recordings directly in response to transcutaneous TI stimulation. Similarly, the available literature on the neural response to sine wave stimulation is sparse, despite some research suggesting its improved selectivity to different types of fibres based on the frequency used [10], [11].

The aim of this paper is, therefore, to record and analyse the neural response to temporal interference stimulation and

L.J. (email: lj386@bath.ac.uk), M.R. (email: mr611@bath.ac.uk) and B. W. M. (email: bwm23@bath.ac.uk) are with the Centre for Biosensors, Bioelectronics, and Biodevices (C3Bio), Department of Electronic and Electrical Engineering, University of Bath, Bath BA2 7AY, UK. LJ received funding for this work through the Santander Mobility Award and received sponsorship through the Dr Brian Nicholson scholarship, Antony Best scholarship, the Esther Parkin Trust scholarship as well as the University of Bath through the University Research Studentship Award (URSA).

F. R.A. (email: fran@hst.aau.dk) and T.G.N.d.S.N. (email: thnn@hst.aau.dk) are with the Center for Neuroplasticity and Pain (CNAP), Department of Health Science and Technology, Aalborg University, 9220 Aalborg, Denmark. CNAP is supported by the Danish National Research Foundation (DNRF121).

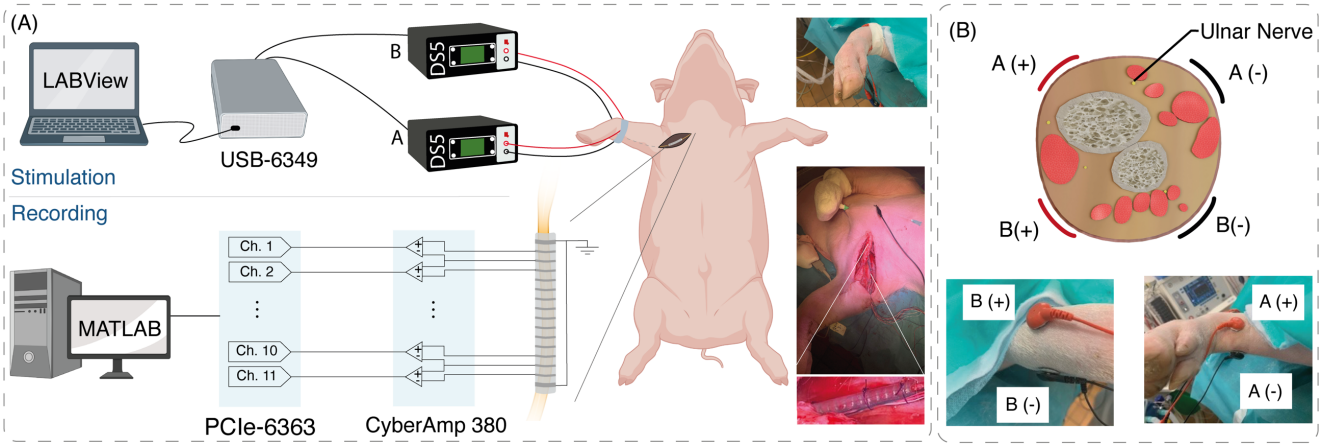

Fig. 1. Experimental setup. A) Stimulation and recording equipment and photos of the electrodes (covered by tape) and incision showing the implanted recording cuff. B) Position of the electrode pairs (A and B) relative to the location of the ulnar nerve and photos of their placement on the animal. This figure was partially created using BioRender.com.

compare it to sine wave stimulation at the same current levels. Being the first recording of this type, this work also highlights some of the difficulties associated with recording ENG signals when using high-frequency sinusoidal stimulation waveforms. Thus, the presented results provide a starting point to investigate TI stimulation at a new intermediate level to aid with the complete understanding of its mechanisms.

II. Methods

A. Surgical Approach

The following procedure was performed in accordance with the Danish Veterinary and Food Administration under the Ministry of Food, Agriculture and Fisheries of Denmark (protocol number 2017-15-0201-01317) . A Female Landrace pig weighing ~34.5 kg was anaesthetised using sevoflurane (1.5 to 2.5% minimum alveolar concentration), propofol (2 mgh^{-1} kg^{-1}), and fentanyl (10 μg h^{-1} kg^{-1}), and mechanically ventilated at 15 cycles per minute.

A 20 cm incision was used to expose the ulnar nerve which was dissected free from its point of bifurcation (near the shoulder) until inaccessible distally (near the elbow). A multiple-electrode recording cuff (see section C) was implanted on the nerve. Anaesthesia was reduced after the surgery, and the pig was allowed to stabilise its physiological parameters before innervation mapping was carried out.

B. Electrical Stimulation

A custom LabVIEW (National Instruments, Austin, TX, USA) program was used to run sweeps of sinusoidal stimulations with varying amplitude (1mA steps) and frequency, as shown in Table 1 with a 1.5 s gap between different stimulation runs. The program generated the waveforms at a sampling rate of 80 kS/s, and a USB data acquisition device (USB-634z9, National Instruments, Austin, TX, USA) was used to output those waveforms to two isolated bipolar constant-current stimulators (DS5, Digitimer, Hertfordshire, UK).

Ag/AgCl electrodes of approximately 1.8 cm diameter were placed on the pig skin at the locations shown in Fig. 1 (B). Surgical tape was used to improve the adhesion of the electrodes to the skin. Each pair of electrodes (A and B) was connected to a separate stimulator to enable simultaneous stimulation (sweeps 7 to 9, Table 1).

TABLE I. Summary of Sweeps

Sweep #	F_A (Hz)	I_A (mA)	F_B (Hz)	I_B (mA)	Duration (s)
1	100	$1 \rightarrow 5$	-	-	0.1
2	-	-	100	$1 \rightarrow 5$	0.1
3	2000	$1 \rightarrow 5$	-	-	0.1
4	-	-	2000	$1 \rightarrow 5$	0.1
5	4000	$1 \rightarrow 5$	-	-	0.1
6	-	-	4000	$1 \rightarrow 5$	0.1
7	100	$1 \rightarrow 4$	100	$4 \rightarrow 1$	1
8*	2000	$1 \rightarrow 4$	2100	$4 \rightarrow 1$	1
9*	4000	$1 \rightarrow 4$	4100	$4 \rightarrow 1$	1

F_A and F_B are the frequencies of stimulation and I_A and I_B are the peak amplitudes for channels A and B, respectively.* indicates TI stimulations.

The maximum stimulation current range was initially chosen to reach 10mA. The full sweeps were run once to observe muscle activation. However, the limit had to be reduced to 5 mA to prevent amplifier saturation at high frequencies and allow for ENG recording.

C. Recording

A 50mm recording cuff (shown in Fig. 1 (A)) was manufactured in accordance with the process described in [12]. The cuff consisted of 12 electrodes (width = 0.5 mm) between 2 guard electrodes (width =1 mm), with an inter-electrode distance of 3.5 mm. A subcutaneous stainless-steel probe was used to ground the animal. This ground was shared with the amplifiers and stimulators. The recording cuff was connected to a CyberAmp 380 amplifier bank and AI402 SmartProbes, both from Axon Instruments Inc. The cuff was configured for bipolar recordings (see Fig 1 (A) and [13]). The total amplifier gain was 25,000 (limited by stimulation artefacts), and the data was digitised using a PCIe-6363 card (National Instruments) at a sampling frequency of 90 kS/s with a 16-bit resolution.

D. Data Analysis

The data was first visually inspected to note any channels with recording errors (e.g., saturated). Those channels were not included in the analysis process. The digitalised data was pre-processed to remove stimulation artefacts using an optimisation function in MATLAB (*fminsearch*) where the

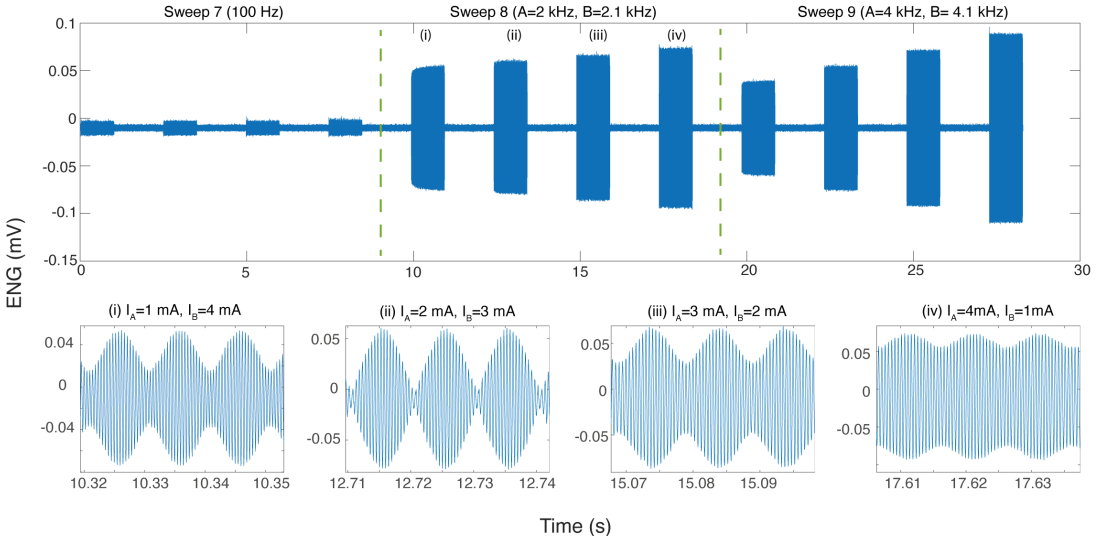

Fig. 2. The top plot shows how stimulation artefact magnitude increases with stimulation frequency. The bottom row plots show how the stimulation artefact provided an indicator of the depth of modulation experienced with different ratios of currents between channel A and B.

Nelder—Mead simplex method [14] is used to select the amplitude, phase, and offset of the sinusoidal waveform(s) based on the known stimulation frequency. The estimated stimulation artefact waveform was then subtracted from the recorded signal. The resulting signal was then bandpass filtered using an eighth order Butterworth filter with cut-off frequencies of 300 Hz and 8 kHz.

The filtered data was normalised then analysed using the *delay-and-add* algorithm, which has been shown to improve the SNR by $\sqrt{C}$ where C is the number of electrode channels (C=7 after eliminating channels with recording errors). The processes involved artificially delaying the recording channels relative to the first electrode [15]. This delay is proportional to the distance between the electrodes and was swept across values corresponding to conduction velocities between 30 m/s and 100 m/s in 400 steps. The *delay-and-add* process was carried out in the frequency domain (to increase computational efficiency [16]), and the recordings corresponding to the faulty electrodes were replaced with infinitesimal values. Once the data has been transformed into the velocity-time domain, an image processing approach was used to detect action potentials by representing the data as a velocity by time image and using MATLAB's *watershed* function and a threshold of 10 dB to identify the bright spots corresponding to detected spikes [16].

III. Results

A. Muscle response with high currents

Clear muscle responses were observed at currents above 5 mA, with sweeps 1 and 2 resulting in limb movements in opposite directions. Sweep 7 showed the effect of current steering as the direction of muscle activation switched during the sweep. No muscle activation was observed for the remaining sweeps.

B. Stimulation artefact

Despite the distance between the stimulation site and recording electrodes (>15 cm), large stimulation artefacts were present in the recordings. The magnitude of the artefacts was significantly greater at high frequencies, as shown in Fig. 2 and resulted in amplifier saturation. The shape of the stimulation artefact matched the stimulation waveform enabling their removal by subtracting the estimated artefact waveform based on the known stimulation frequency (see section II D and Fig. 3 (A)).

The stimulation artefacts during temporal interference stimulation provided an indication of the modulation depth at the nerve location. Fig.2 shows that as the current is steered from A to B, the depth of modulation varied in accordance with expectations based on the literature. Given that the ulnar nerve is closer to electrode pair A, the maximum depth of modulation occurs when I_B is higher than I_A, allowing the magnitude of the sine waves reaching the nerve from both sources to be equal.

C. Sine wave stimulation

The recordings matched what has been reported in [17], showing what looks like compound action potentials (CAPs) at times roughly correlated to the peaks and troughs of the sine wave stimulation (see Fig. 3 (A) i), with stronger responses at the peaks. An example is shown in Fig. 3 (B), where increased stimulation current corresponded to an increase in the number and size of the CAP-like response. Those responses were seen across the entirety of sweeps 1, 2 and 7, with the response in sweep 2 being weaker than the other two sweeps.

D. Temporal interference stimulation

Repeating the signal processing procedure with the recordings from the temporal interference stimulation sweeps (8 and 9) did not result in a clearly visible neural response. However, the delay-and-add process was able to detect spikes that, upon inspection and despite the low SNR, looked like neural responses propagating across the length of the electrode (see Fig. 4).

The detected spikes were randomly spread across the recording and did not correlate to the peaks or troughs of the modulation envelope. Moreover, no consistent trend was observed in relation to the number of spikes relative to the depth of modulation. Fig. 3 (C) shows an example of two velocity vs time plots obtained for maximum (i) and minimum

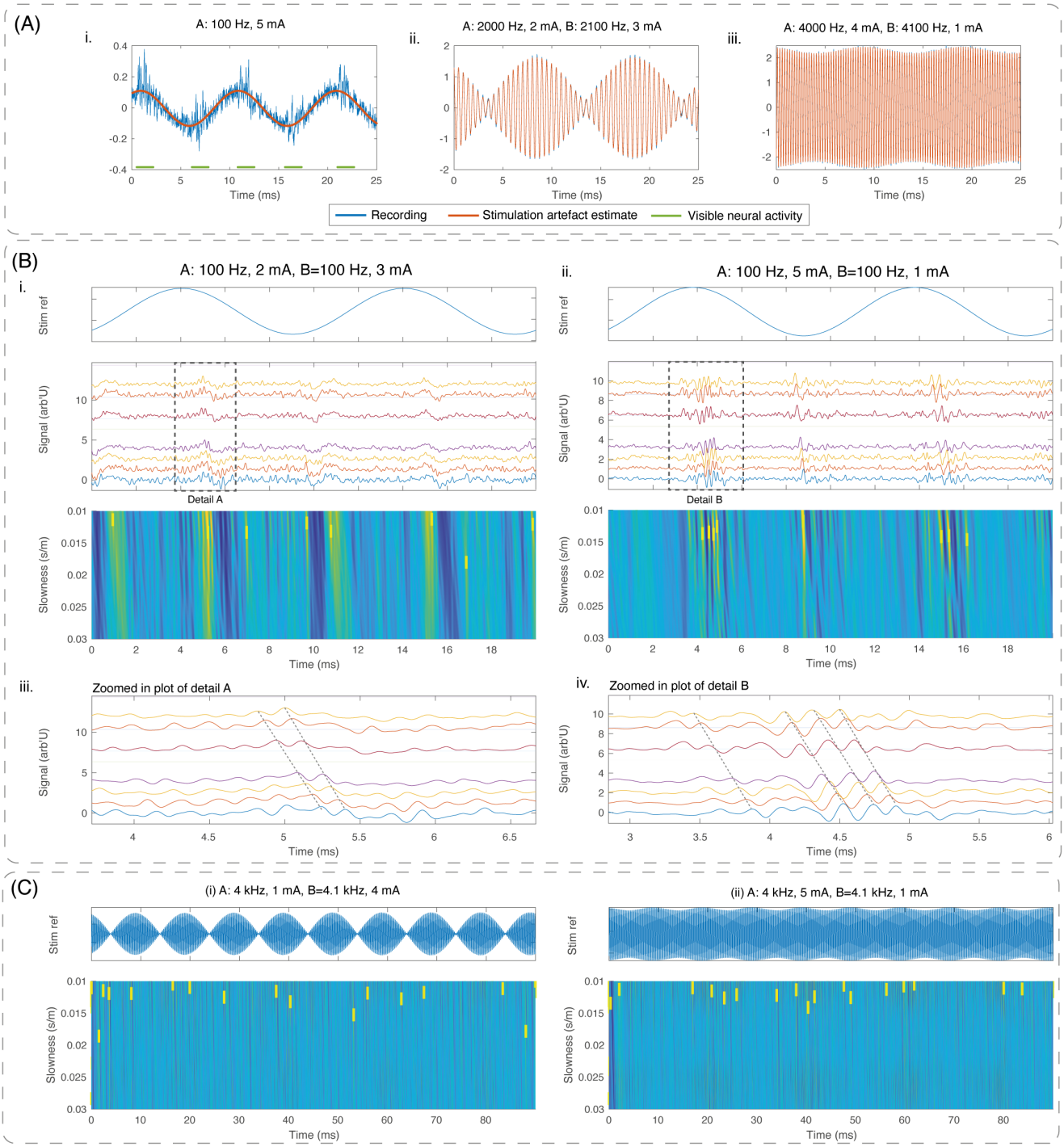

Fig. 3. (A) Stimulation artefact removal examples for different frequencies (B) Section of the recording from sweep 7 showing CAP-like activity at times correlating to the peaks and troughs of the sine wave stimulation. The plots starting from the top are 1) The estimate stimulation artefact 2) the normalised recordings from the different channels stacked to show propagation. The non-uniform spacing at some locations is due to the removal of some channels from the processing step. 3) Slowness vs time plot highlighting the identified spikes with yellow markers. 4) a zoomed-in version of the details highlighted in (2) to show propagation. (C) comparison of the slowness vs time plot obtained with maximum and minimum depths of modulation in sweep 9.

depths of modulation (ii). For comparison, equivalent plots were produced for sweep 4 and for recordings when no stimulation was applied (not presented) and showed similar spontaneous firing patterns.

IV. Discussion

This work provides a starting point for developing experimental procedures to record the neural response during temporal interference stimulation. While effectively removable through the described optimisation process, the stimulation artefact proved to be the primary technical limitation of this procedure, resulting in amplifier saturation.

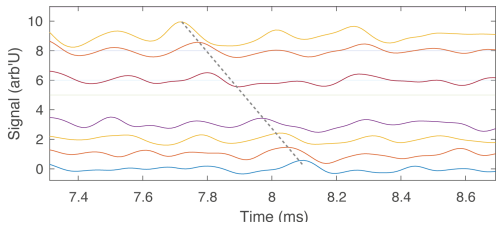

Fig. 4. Example recordings corresponding to a detected spike from sweep 9 with I_A= 1mA and I_B=4 mA following the same approach in Fig. 3 (b) iii and iv.

The magnitude of the artefact during kHz sinusoidal stimulation was much greater than during 100 Hz sinusoidal stimulation and typical magnitudes observed with square-wave stimulation (root mean square values of 15-85, 3-5, and few μV [18], respectively). The amplifier gain had to, therefore, be reduced, lowering the SNR. A potential solution to overcome the presence of sinusoidal artefacts is to incorporate narrow bandstop filters within the hardware with cut-off frequencies corresponding to the stimulation frequency. Moreover, the reported magnitudes of stimulation artefact and neural response patterns can be referred to when designing similar experiments.

The low-frequency sinusoidal stimulation results matched expectations by showing activation that followed the peaks and troughs of the stimulation waveform. The use of the *delay-and-add* algorithm showed the propagation of the CAP-like response through the nerve at conduction velocities similar to those that have been reported previously for pig ulnar nerves [19], increasing the confidence in it being a neural response.

Despite the stimulation artefact showing maximum amplitude modulation in some temporal interference stimulation recordings, the neural response did not correlate to the 100 Hz envelope. Moreover, no correlation was found between the number of spikes detected and the level of amplitude modulation. One explanation for the detected spikes is that they are due to spontaneous neural activity, unrelated to the temporal interference stimulation. This assumption was further supported by the presence of a similar response with pure sinusoidal high-frequency stimulation and in recordings with no electrical stimulation applied. Those results suggest that, despite the increased penetration, temporal interference stimulation may not result in neural activation when used at current amplitudes comparable to low-frequency stimulation. This result is in line with previous computational modelling work [3], [7] suggesting that TI stimulation requires higher current amplitudes compared to low-frequency stimulation.

V. Conclusion

This paper presented ENG recordings made from the ulnar nerve of a pig in response to TI stimulation and sine wave stimulation at matching current levels. Being the first recording of this type, this work showed that high-frequency stimulation waveforms result in significantly larger stimulation artefacts than those experienced with lower frequencies, leading to amplifier saturation. The results showed a clear neural response with 100 Hz sine wave stimulation but no correlation between TI stimulation and detected spikes in the neural recording was found, suggesting that higher currents may be required. Thus, the presented results provide a starting point to develop dedicated experimental methods to investigate the effect of TI stimulation on the neural response through ENG recordings.

References

[1] G. C. Goats, "Interferential current therapy," *Br. J. Sports Med.*, vol. 24, no. 2, pp. 87–92, 1990,

[2] N. Grossman *et al.*, "Noninvasive Deep Brain Stimulation via Temporally Interfering Electric Fields," *Cell*, vol. 169, no. 6, pp. 1029-1041.e16, 2017,

[3] L. Jabban, D. Zhang, and B. W. Metcalfe, "Interferential Current Stimulation for Non-Invasive Somatotopic Sensory Feedback for Upper-Limb Prosthesis: Simulation Results using a Computable Human Phantom," in *2021 10th International IEEE/EMBS Conference on Neural Engineering (NER)*, May 2021, pp. 765–768.

[4] R. C. Venancio, S. Pelegrini, D. Q. Gomes, E. Y. Nakano, and R. E. Liebano, "Effects of Carrier Frequency of Interferential Current on Pressure Pain Threshold and Sensory Comfort in Humans," *Arch. Phys. Med. Rehabil.*, vol. 94, no. 1, pp. 95–102, Jan. 2013,

[5] M. D. Sunshine *et al.*, "Restoration of breathing after opioid overdose and spinal cord injury using temporal interference stimulation," *Commun. Biol. 2021 41*, vol. 4, no. 1, pp. 1–15, Jan. 2021,

[6] E. Mirzakhalili, B. Barra, M. Capogrosso, and S. F. Lempka, "Biophysics of Temporal Interference Stimulation," *Cell Syst.*, pp. 1–16, 2020,

[7] B. Howell and C. C. McIntyre, "Feasibility of Interferential and Pulsed Transcranial Electrical Stimulation for Neuromodulation at the Human Scale," *Neuromodulation*, vol. 2020, 2020,

[8] Z. Esmaeilpour, G. Kronberg, D. Reato, L. C. Parra, and M. Bikson, "Temporal interference stimulation targets deep brain regions by modulating neural oscillations," *Brain Stimul.*, vol. 14, no. 1, pp. 55–65, Jan. 2021,

[9] B. Barra, V. Paggi, S. Lacour, M. Capogrosso, and L. Fisher, "Amplitude Modulated High-Frequency Stimulation Elicits Stochastic Axonal Spiking Activity," 2021.

[10] S. Sundar and J. A. González-Cueto, "On the activation threshold of nerve fibers using sinusoidal electrical stimulation," *Annu. Int. Conf. IEEE Eng. Med. Biol. - Proc.*, pp. 2908–2911, 2006,

[11] D. K. Freeman, D. K. Eddington, J. F. Rizzo, and S. I. Fried, "Selective activation of neuronal targets with sinusoidal electric stimulation," *J. Neurophysiol.*, vol. 104, no. 5, Nov. 2010,

[12] M. Haugland, "Flexible method for fabrication of nerve cuff electrodes," *Annu. Int. Conf. IEEE Eng. Med. Biol. - Proc.*, no. 1, pp. 359–360, 1996,

[13] B. W. Metcalfe, D. J. Chew, C. T. Clarke, N. de N. Donaldson, and J. T. Taylor, "A new method for spike extraction using velocity selective recording demonstrated with physiological ENG in Rat," *J. Neurosci. Methods*, vol. 251, pp. 47–55, Aug. 2015,

[14] J. C. Lagarias, J. A. Reeds, M. H. Wright, and P. E. Wright, "Convergence Properties of the Nelder--Mead Simplex Method in Low Dimensions," *SIAM J. Optim.*, vol. 9, no. 1, pp. 112–147, Jul. 2006,

[15] J. Taylor, M. Schuettler, C. Clarke, and N. Donaldson, "The theory of velocity selective neural recording: a study based on simulation," *Med. Biol. Eng. Comput.*, vol. 50, no. 3, pp. 309–318, Mar. 2012,

[16] B. W. Metcalfe, A. J. Hunter, J. E. Graham-Harper-Cater, and J. T. Taylor, "Array processing of neural signals recorded from the peripheral nervous system for the classification of action potentials," *J. Neurosci. Methods*, vol. 347, p. 108967, Jan. 2021,

[17] B. Wodlinger and D. M. Durand, "Peripheral nerve signal recording and processing for artificial limb control," *Annu. Int. Conf. IEEE Eng. Med. Biol. Soc. IEEE Eng. Med. Biol. Soc. Annu. Int. Conf.*, vol. 2010, pp. 6206–6209, 2010,

[18] J. L. Parker, N. H. Shariati, and D. M. Karantonis, "Electrically evoked compound action potential recording in peripheral nerves," *Bioelectron. Med.*, vol. 1, no. 1, pp. 71–83, Jan. 2018,

[19] F. R. Andreis *et al.*, "The Use of the Velocity Selective Recording Technique to Reveal the Excitation Properties of the Ulnar Nerve in Pigs," *Sensors*, vol. 22, no. 1, Dec. 2021,